POLITECNICO DI TORINO
Repository ISTITUZIONALE

Experimental Testing and Identification of Bistable Systems for Seismic Energy Dissipation

Original
Experimental Testing and Identification of Bistable Systems for Seismic Energy Dissipation / Scussolini, L., Cavanni, V., Lorefice, P., Surace, C., Ceravolo, R.. - In: THE E-JOURNAL OF NONDESTRUCTIVE TESTING. - ISSN 1435-4934. - 31:(2026), pp. 1-9. (12th European Workshop on Structural Health Monitoring (EWSHM 2026) Toulouse (France) July 7-10, 2026) [10.58286/33701].

Availability:
This version is available at: 11583/3014567 since: 2026-08-17T12:10:41Z

Publisher:
NDT.net

Published
DOI:10.58286/33701

Terms of use:

This article is made available under terms and conditions as specified in the corresponding bibliographic description in the repository

Publisher copyright

(Article begins on next page)

01 November 2026

More info about this article: https://www.ndt.net/?id=33701

Experimental Testing and Identification of Bistable Systems for Seismic Energy Dissipation

Linda SCUSSOLINI [1], Valeria CAVANNI [1], Paolo LOREFICE [1], Cecilia SURACE [1], Rosario CERAVOLO [1,2]

[1] Department of Structural, Geotechnical, and Building Engineering, Politecnico di Torino, Corso Duca degli Abruzzi, 24, 10129 Turin, Italy; Email: linda.scussolini@polito.it, valeria.cavanni@polito.it, paolo.lorefice@studenti.polito.it, cecilia.surace@polito.it, rosario.ceravolo@polito.it

[2] Responsible Risk Resilience interdepartmental Centre (R3C), Politecnico di Torino, Corso Duca degli Abruzzi, 24, 10129 Turin, Italy

Abstract. The identification of dynamic parameters in nonlinear systems is a challenging task, particularly when dealing with experimental measurements. If the nonlinearity is negligible for the response, one can rely on linear techniques without compromising the accuracy of the solution. However, if the nonlinear effects are significant, as frequently happens under strong excitations, these assumptions do not hold anymore, and one should refer to more sophisticated methods. This is the case of bistable systems, i.e., systems characterised by two stable equilibria and one unstable equilibrium point. In experimental settings, additional uncertainties may arise from the definition of boundary conditions, materials, and manufacturing. In this context, the need for a technique capable of instantaneously tracking the nonlinear parameters of systems exhibiting rapid changes, such as the bistable ones, is fundamental. This requirement is mainly linked to the ultimate purpose of these systems, namely the dissipation and/or absorption in terms of instantaneous energy, which is critical in real-world applications. This work describes a novel method for experimentally measuring and identifying dynamic parameters of bistable systems. An instantaneous probabilistic estimator, constructed using an unscented Kalman filter (UKF), is proposed for the identification of the parameters governing the bistable dynamics. The method is validated by employing experimental measurements achieved during a testing campaign carried out on a 3D-printed bistable sample, with the final goal of estimating the instantaneous energy dissipated under different external excitations. To this end, an ad hoc testing machine, composed of a pendulum actuator, was built to accurately simulate the single degree-of-freedom model employed in the identification task. The procedure proved robust and reliable.

Keywords: Nonlinear identification, Experimental testing, Bistable systems, Probabilistic approaches

Introduction

In its broadest sense, nonlinear identification consists of fitting data into nonlinear models, similarly to its linear counterpart. Throughout the years, several techniques have been proposed and developed to overcome the nonlinear identification problem [1–3]. However, when dealing with experimental settings, the difficulties related to a proper estimation of nonlinear parameters increase, and the need for more sophisticated techniques arises. When the system under consideration remains under operational conditions, the nonlinear effects can be considered as negligible, and a convenient choice is to rely on linear techniques. However, there are cases, especially in the presence of extreme events,

This work is licensed under CC BY 4.0

Media and Publishing Partner NDT.net
https://doi.org/10.58286/33701

e.g., earthquakes, where this assumption does not hold anymore and one should employ more sophisticated nonlinear techniques.
This is the case of systems characterised by two stable equilibria and one unstable equilibrium point, namely bistable systems. If properly excited, these systems oscillate between the two stable positions, leading to convenient properties, such as energy dissipation, especially if coupled with linear oscillators, e.g., frames [4]. However, the experimental testing of these elements is a challenging task. This is due to the fact that additional uncertainties may arise from the definition of boundary conditions, materials, and manufacturing, which complicate the interpretation of the nonlinear behaviour.
To this end, an appealing choice is to estimate instant by instant the properties of the system, in order to take into account any possible change in the ideal testing conditions. Instantaneous techniques have been employed primarily in the field of structural health monitoring (SHM) for damage detection purposes, but they proved effective also in nonlinear identification tasks [5]. Instantaneous nonlinear identification methods can be further divided into online and offline. Offline methods are mainly based on the Hilbert transform [6,7]. Among online methods, Bayesian filters, such as the extended Kalman filter (EKF) [8] and unscented Kalman filter (UKF) [9], represent a compelling category. Particularly, the UKF has the advantage of overcoming the linearisation errors of the EKF while simultaneously reducing the computational complexity.
For bistable systems subject to rapid changes, it is essential to track nonlinear parameters instantaneously [10,11]. This allows for optimisation of instantaneous energy dissipation/absorption, which are crucial for testing the system effectiveness in operational environments. In light of these considerations, this work describes a novel method for experimentally measuring and identifying nonlinear parameters of bistable systems. An instantaneous probabilistic estimator is implemented for the identification of the parameters governing the bistable dynamics. In particular, the UKF is combined with a Markov Chain Monte Carlo (MCMC) sampling to account for uncertainties. The method is validated both numerically and experimentally, employing measurements achieved during a testing campaign carried out on a 3D-printed bistable sample. To this end, an ad hoc testing machine, composed of a pendulum actuator, was built to accurately simulate the single degree-of-freedom model employed in the identification task.
The paper is structured as follows. Section 1 describes the process from the conceptualisation to the laboratory testing of an in-scale bistable sample of a seismic energy dissipation device. In Section 2 an overview on the implementation of the combined UKF-MCMC, built starting from [12], is provided. Section 3 reports the nonlinear parameter estimation results, first from a numerical standpoint, then employing the experimental signals gathered from the testing machine described in Section 2, also discussing the effectiveness of the device in terms of instantaneous dissipated energy. Section 4 discusses and concludes this work.

1. Bistable devices for seismic energy dissipation: from conceptualisation to testing

Structures situated in seismic-prone areas require robust mitigation strategies to ensure their structural integrity. Beyond conventional base isolation, one may exploit seismic energy dissipation/absorption through specific devices. A common example is represented by the tuned mass damper (TMD), which mitigates the displacement by coupling a secondary mass to specific vibration modes. Recent advancements have transitioned these devices into their nonlinear counterparts, namely nonlinear energy sinks (NES), to enhance performance by exploiting nonlinear phenomena [13,14]. Among others, bistability is explored to overcome the spatial and mass constraints of traditional TMDs. The rapid transition between the two stable equilibrium states generates high-velocity motion that allows the use of significantly smaller masses compared to conventional TMDs. However, achieving effective bistability requires precise geometric optimisation [15]. By employing an optimised cosine-shaped beam (CSB) [16], it is possible to induce non-conventional characteristics such as a negative elastic modulus, which is particularly effective for energy dissipation. To simulate the device in a scaled version, a decision was made to create a sample using 3D printing technology. The printer used for this purpose is the BambuLab X1 Carbon (https://bambulab.com/it-it/x1). The material used for this process is ABS, which ensures the appropriate rigidity required to achieve bistable behaviour.

This work is licensed under CC BY 4.0

Media and Publishing Partner NDT.net

The CSB made of ABS can be conveniently represented by a nonlinear single-degree-of-freedom (SDoF), described by the following equation of motion:

$$m\ddot{y} + c\dot{y} + k_1 y + k_3 y^3 = u(t) \quad (1)$$

where m is the mass of the system, c is the linear damping, k_1 is the negative linear stiffness, and k_3 is the positive cubic stiffness. The system exhibits a displacement y under the generic external excitation $u(t)$. The requirement $k_1 < 0$ is needed to achieve bistability. In steady-state, the system has three solutions, $y_0 = \pm\sqrt{-k_1/k_3}$, i.e., the stable equilibrium points, and $y_0 = 0$, i.e., the unstable equilibrium point. When the system oscillates around the stable equilibrium points, it is said to exhibit *intrawell* oscillations. Conversely, when it jumps between the two configurations, it is said to exhibit *interwell* oscillations [17]. A representation of the bistable device and its schematic are provided in **Fig. 1**, while **Table 1** lists the parameters of the 3D-printed sample.

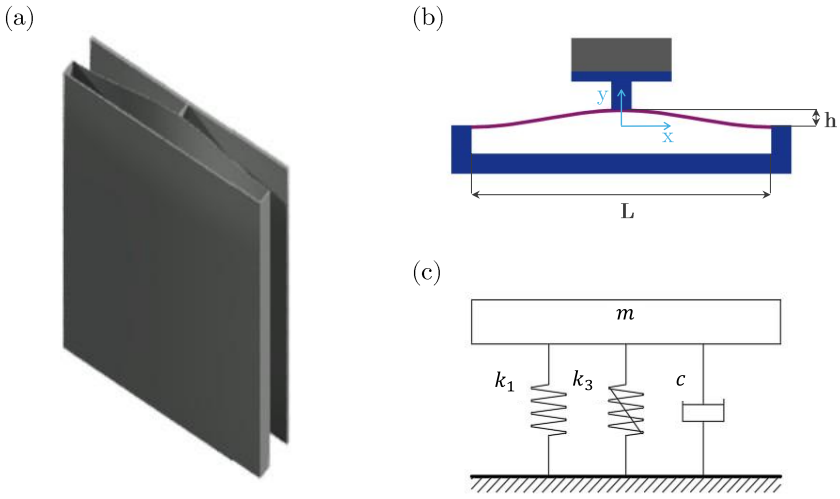


Fig. 1. (a) 3D representation of the device, (b) schematic for fabrication, and (c) equivalent SDoF oscillator.

Table 1. Properties of the in-scale sample of the bistable device.

Property	**Value**
Height h [m]	6.00×10^{-3}
Thickness t [m]	1.00×10^{-3}
Length L [m]	9.00×10^{-2}
Elastic modulus E [MPa]	2.20×10^{3}
Density ρ [kg/m^3]	1.05×10^{3}

The prototype testing machine is composed of a high-precision measurement and actuation system, isolated from external vibrations by a solid granite base. The measurement system is based on a HeNe laser beam, shaped by cylindrical lenses and 45° mirrors. The light beam is focused on a 12-mm-long linear position sensitive detector. This sensor detects the displacement of the vibrating mass with an uncertainty of less than 50 µm, exploiting the photocurrent distribution generated by the light beam impact. Actuation is performed by an electromagnetic system composed of copper coils with a total of 40 turns and 1 T neodymium permanent magnets, powered by a 20 A amplifier to perform both free decay and forced tests. To prevent rotational or transverse vibration modes, ensuring the SDoF formulation of Eq. (1), the testing machine is stiffened by four tensile tie rods and equipped with a steel plate pendulum that restrains the pusher. A detailed representation of the actuation and measurement system is given in **Fig. 2**, while the testing machine is depicted in **Fig. 3**.

This work is licensed under CC BY 4.0

Media and Publishing Partner NDT.net

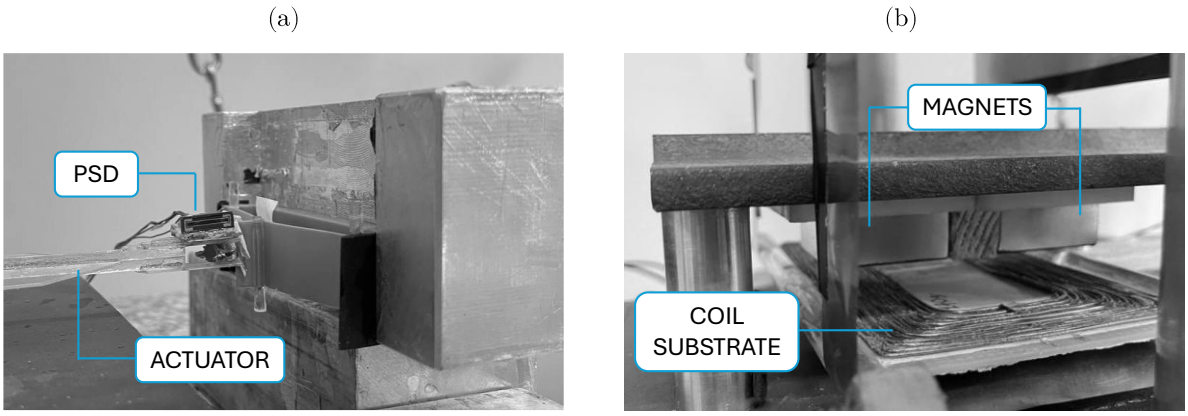


Fig. 2. Details of the actuation and measurement system. (a) Actuator and position sensitive detector (PSD). (b) Coil substrate and magnets.

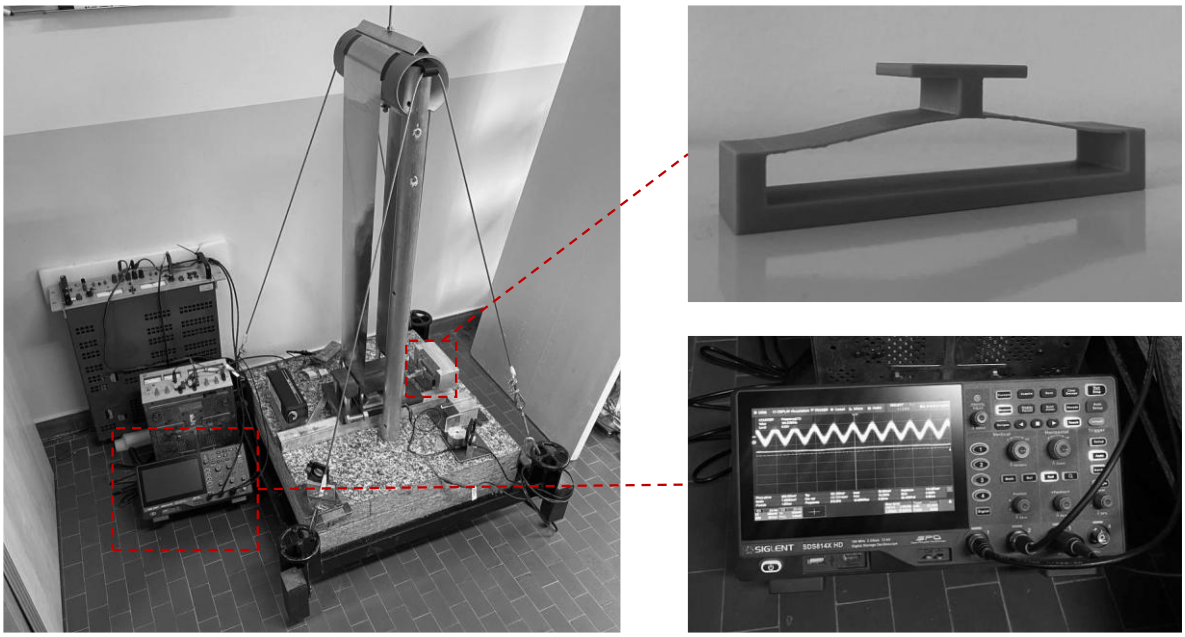


Fig. 3. Testing machine equipped with pendulum actuator. Details of the sample and the oscilloscope.

2. A modified version of unscented Kalman filter (UKF) for nonlinear identification

This section briefly describes a modified version of the UKF for the sequential estimation of states and parameters in nonlinear dynamical systems. Bayesian approaches have proved effective in the identification of nonlinear systems [18]. In this case, the MCMC method is employed. The MCMC basically relies on the idea of building a chain of values progressively exploring the parameter space in such a way that, after a certain number of iterations, the sample distribution coincides with the desired posterior distribution. It is therefore a stochastic and iterative process, in which every state depends only on the previous state, based on the Markov principle. The Metropolis-Hastings is one of the most common MCMC algorithms for generating samples from a target distribution. Unlike traditional Monte Carlo methods, the Metropolis-Hastings algorithm employs a density depending on the current state of the chain, avoiding the loss of efficiency typical of such methods.
However, the MCMC method does not allow instantaneous evaluation of the parameters to be estimated, which is advantageous in the case of systems showing rapid changes in the response. To this end, it has been combined with one of the methods enabling instantaneous implementation, and thus suitable for time-varying responses. In its classical implementation, the UKF consists of two

This work is licensed under CC BY 4.0

Media and Publishing Partner NDT.net

steps, namely prediction and correction. The equations of a general dynamic system can be defined by resorting to the state-space equation and its measurement equation as follows:

$$\mathbf{x}_k = f(\mathbf{x}_{k-1}, u_{k-1}) + \mathbf{q}_k \quad (2)$$

$$\mathbf{y}_k = h(\mathbf{x}_k) + \mathbf{r}_k \quad (3)$$

where $\mathbf{x}$ is the state vector in its augmented form, $\mathbf{y}$ is the output vector, and u is the external input excitation. The vectors $\mathbf{q}$ and $\mathbf{r}$ are the process and measurement noises, respectively. The state vectors are augmented to take also into account the parameters to be estimated in the identification process. An overview of the algorithm employed in this work can be found in [19,20].
Here, starting from [12], a similar algorithm, which combines the UKF as proposed by [19] and a Metropolis-Hastings MCMC, has been implemented. Differently from [12], the proposed approach introduces a sequential UKF-MCMC algorithm that produces a temporal distribution of the parameters with an adaptive MCMC step automatically tuned as a function of a predefined acceptance rate. The pseudocode of the algorithm is reported in Algorithm 1.

Algorithm 1: UKF-MCMC algorithm

Initialisation:
Log-transform mapping $\mathbf{T}$
Log-parameters $\boldsymbol{\phi}$
Augmented state vector $\mathbf{x}_k$
Gaussian prior on log-parameters $\boldsymbol{\phi} \sim N(\boldsymbol{\mu}_{\boldsymbol{\phi}}, \boldsymbol{\Sigma}_{\boldsymbol{\phi}})$
for $t_k = 1{:}\,t_N$
  $\mathbf{x}_k = f(\mathbf{x}_{k-1}, u_k)$ — Prediction
  $\hat{\mathbf{y}}_k = h(\mathbf{x}_k), \mathbf{x}_k = \mathbf{x}_k + \mathbf{K}_k(\mathbf{y}_k - \hat{\mathbf{y}}_k)$ — Updating
  for $s = 1, \ldots, N_{MCMC}$
    $\boldsymbol{\phi}^* = \boldsymbol{\phi}^{(s-1)} + \boldsymbol{\varepsilon}_s$ with $\boldsymbol{\varepsilon}_s \sim N(0, \boldsymbol{\Sigma}_{\mathbf{q}})$ — Proposed distribution
    $\log p^* = \log p\,(\boldsymbol{\phi}^* | \mathbf{y}_{1:k})$ — Proposed log-posterior
    $\log p^{(s-1)} = \log p\,(\boldsymbol{\phi}^{(s-1)} | \mathbf{y}_{1:k})$ — Current log-posterior
    $\alpha = min\{1, \exp(\log p^* - \log p^{(s-1)})\}$ — Acceptance coefficient
    $w \sim U(0,1)$ — Extract sample
    if $w < \alpha$
      $\boldsymbol{\phi}^{(s)} = \boldsymbol{\phi}^*$
    else
      $\boldsymbol{\phi}^{(s)} = \boldsymbol{\phi}^{(s-1)}$
    end
    $\mathbf{p}^{(s)}(t_k) = \mathbf{T}^{-1}\boldsymbol{\phi}^{(s)}$
  end
  $\bar{\mathbf{p}}(t_k) = \frac{1}{N_{MCMC}} \sum_{s=1}^{N_{MCMC}} \mathbf{p}^{(s)}(t_k)$ — Posterior mean
  $\boldsymbol{\phi}_k = \mathbf{T}(\bar{\mathbf{p}}(t_k))$ — Update initial state
end

For the application considered in this work, Algorithm 1 is used to estimate the nonlinear parameters k_1 and k_3 of the bistable SDoF oscillator reported in Eq. (1), yielding $\boldsymbol{\phi} = [\log(-k_1), \log(k_3)]$. It is worth noting that Algorithm 1 can be extended to configurations with multiple DoFs (e.g., including possible rotational effects observed under different testing conditions) by augmenting the state vector. However, such an extension is expected to significantly increase the computational cost associated with the MCMC sampling stage and the overall estimation procedure. The realisations are based on 100 samples for each parameter and are constructed starting from a likelihood-function on the data and a Gaussian log-prior distribution centred on the measured values. Within this framework, and prior to the parameter estimation process, the structural identifiability of the augmented system was

assessed following the observability-based framework proposed in [21]. For the bistable formulation reported in Eq. (1), the observability-identifiability matrix, built through successive Lie derivatives of the measurement equation, was found to have a full rank equal to the dimension of the augmented state vector, thus confirming local observability/identifiability of the states/parameters.

3. Nonlinear parameters estimation results and discussion

3.1 Numerical validation

First, a numerical validation was carried out to assess the performance of the algorithm. Specifically, white noise with zero mean and standard deviation equal to 5 was employed to simulate the bistable response of the system. The signal has a duration of 20 s with a sampling time of 0.01 s. The values employed in the identification process are listed in **Table 2**. The input and output responses are shown in **Fig. 4**. Results of the identification task are illustrated in **Fig. 5**. In particular, following an initial transient phase in the first two seconds, the parameters k_1 and k_3 tend to stabilise around their theoretical values, while maintaining relatively narrow confidence bounds (see **Fig. 5a**). This convergence is also supported by the trend observable in **Fig. 5b**. Indeed, as the number of MCMC steps increases, the acceptance rate decreases.

Table 2. Numerical values employed for parameter estimation.

Parameter	m [kg]	c [Ns/m]	k_1 [N/m]	k_3 [N/m^3]
Initial value	47×10^{-3}	3.4	-5.5×10^{2}	1.8×10^{7}
Lower boundary	Fixed	Fixed	-5.0×10^{3}	1.0×10^{7}
Upper boundary	Fixed	Fixed	-5.0×10^{2}	1.0×10^{8}

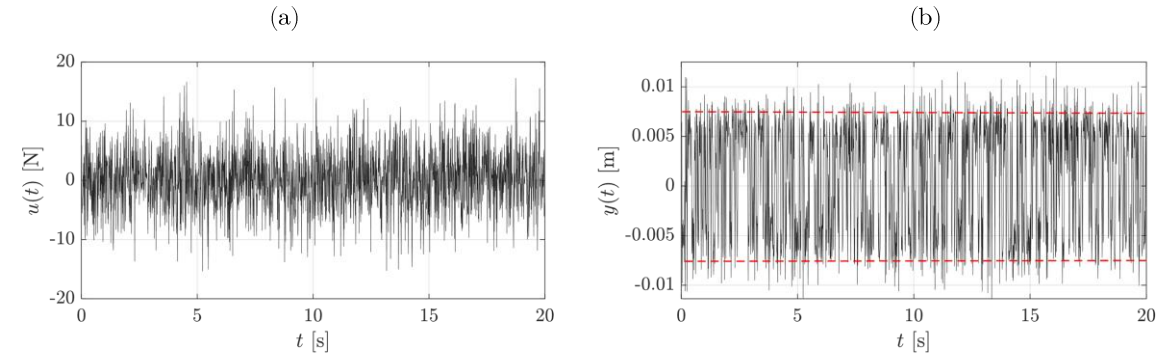


Fig. 4. Numerical simulation: (a) input and (b) system displacement response. The red dotted lines indicate the equilibrium positions.

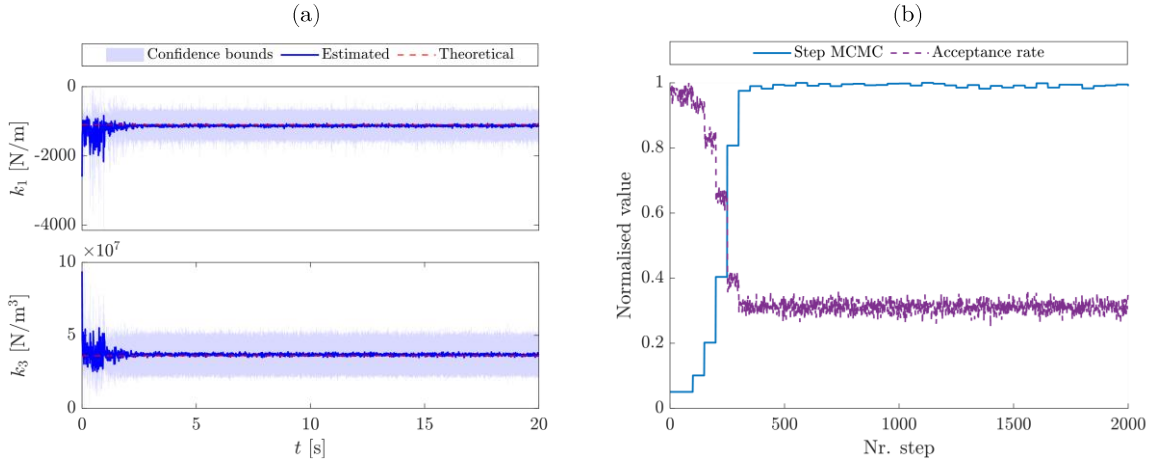


Fig. 5. Numerical simulation: (a) estimated nonlinear parameters and (b) acceptance rate.

This work is licensed under CC BY 4.0

Media and Publishing Partner NDT.net

3.2 Experimental parameter estimation and energy dissipation efficiency assessment

Once the parameter estimation procedure was numerically validated, a response signal gathered through the experimental setup described in Section 2 was employed to characterise the bistable sample with the final purpose of assessing its energy dissipation performance. In this case, the values employed for the identification are listed in **Table 3**. The experimental input and output are displayed in **Fig. 6**. The displacement response signal confirms that the in-scale sample of the device effectively reaches bistability. The system primarily remains in the equilibrium position of $y_0 = 6 \times 10^{-3}$ m, while the jump in the other equilibrium position is induced by the peaks observable in the experimental input. Results are shown in **Fig. 7** and **Fig. 8**. For what concerns parameter estimation, similar results to those obtained in the numerical validation are observable (see **Fig. 7**). More importantly, the dissipated energy progressively increases over time, and a staircase trend is visible when the system jumps from one position to the other (see **Fig. 8b**).

Table 3. Experimental values employed for parameter estimation.

Parameter	m [kg]	c [Ns/m]	k_1 [N/m]	k_3 [N/m^3]
Initial value	205×10^{-3}	5.03	-8.30×10^{2}	3.87×10^{7}
Lower boundary	Fixed	Fixed	-5.00×10^{3}	1.00×10^{7}
Upper boundary	Fixed	Fixed	-5.00×10^{2}	1.00×10^{8}

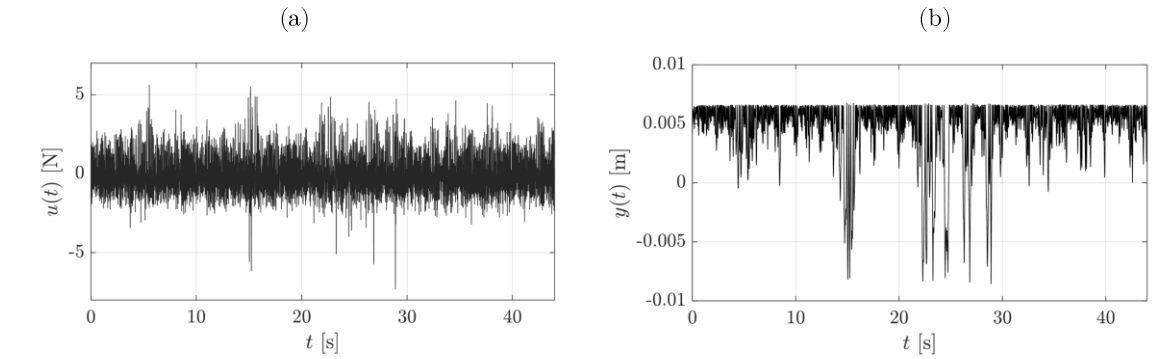


Fig. 6. Experimental testing: (a) white noise input and (b) system displacement response.

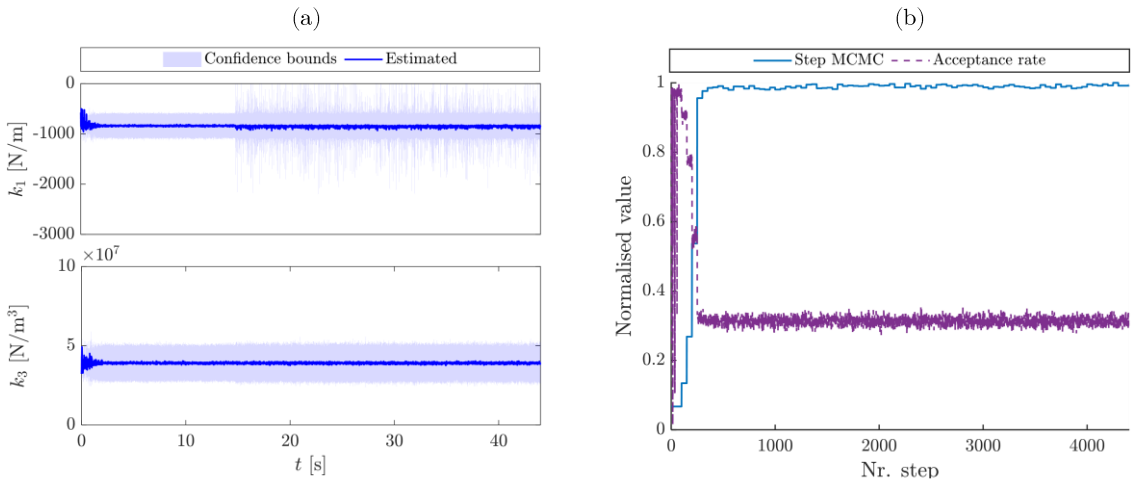


Fig. 7. Experimental testing: (a) estimated nonlinear parameters and (b) acceptance rate.

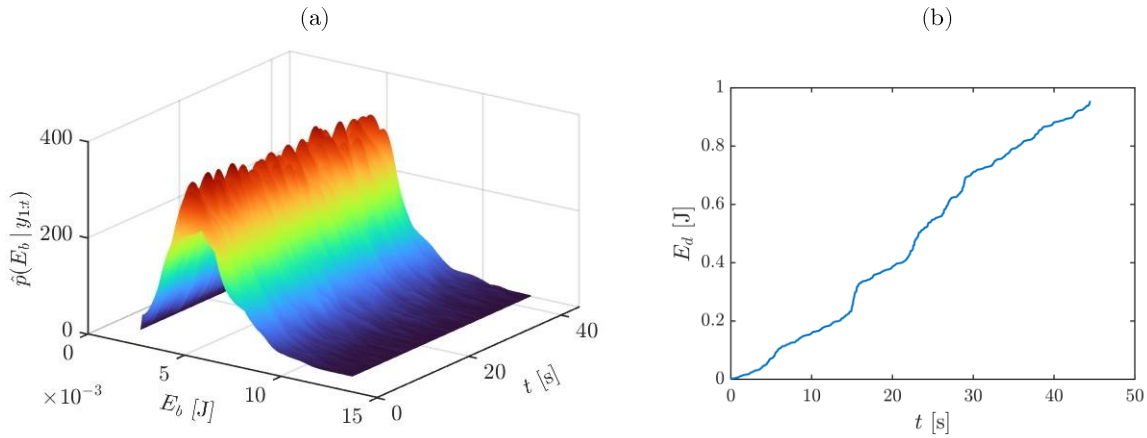


Fig. 8. (a) Energetic barrier and (b) instantaneous dissipated energy over time.

4. Conclusions

This work demonstrates the effective identification of a bistable sample, addressing the inherent challenges of experimental testing uncertainties. The UKF-MCMC estimator, implemented for this purpose, enabled robust estimation of nonlinear parameters from both a numerical and experimental standpoint. Nonlinear data were gathered using a prototype testing machine built ad hoc for the characterisation of bistable samples. The dissipated energy exhibited a staircase trend, where each increment correlates with a snap-through event. This highlights the effectiveness of the device in dissipating energy during interwell transitions, providing a measure of its performance as a passive vibration control system and showing promising capabilities for real-world applications.

Acknowledgements

The research was supported by Fondazione Compagnia di San Paolo, OPTIMISE project, call TRAPEZIO – Paving the way to research excellence and talent. This publication is part of the project PNRR-NGEU, which has received funding from the MUR-DM 118/2023.

References

[1] G. Kerschen, K. Worden, A.F. Vakakis, J.-C. Golinval, Past, present and future of nonlinear system identification in structural dynamics, Mechanical Systems and Signal Processing 20 (2006) 505–592.
[2] J.-P. Noël, G. Kerschen, Nonlinear system identification in structural dynamics: 10 more years of progress, Mechanical Systems and Signal Processing 83 (2017) 2–35.
[3] G. Quaranta, W. Lacarbonara, S.F. Masri, A review on computational intelligence for identification of nonlinear dynamical systems, Nonlinear Dynamics 99 (2020) 1709–1761.
[4] Y. Liu, A. Mojahed, L.A. Bergman, A.F. Vakakis, A new way to introduce geometrically nonlinear stiffness and damping with an application to vibration suppression, Nonlinear Dynamics 96 (2019) 1819–1845.
[5] R. Ceravolo, S. Erlicher, L.Z. Fragonara, Comparison of restoring force models for the identification of structures with hysteresis and degradation, Journal of Sound and Vibration 332 (2013) 6982–6999.
[6] M. Feldman, Hilbert transform applications in mechanical vibration, John Wiley & Sons, 2011.
[7] N.E. Huang, Hilbert-Huang transform and its applications, World scientific, 2014.
[8] M.I. Ribeiro, Kalman and extended kalman filters: Concept, derivation and properties, Institute for Systems and Robotics 43 (2004) 3736–3741.

This work is licensed under CC BY 4.0

Media and Publishing Partner NDT.net

[9] M. Wu, A.W. Smyth, Application of the unscented Kalman filter for real-time nonlinear structural system identification, Structural Control and Health Monitoring: The Official Journal of the International Association for Structural Control and Monitoring and of the European Association for the Control of Structures 14 (2007) 971–990.
[10] L. Scussolini, V. Cavanni, R. Ceravolo, Volterra System Identification Using Wigner-Ville Representations, in: International Conference on Experimental Vibration Analysis for Civil Engineering Structures, Springer, 2025: pp. 281–290.
[11] L. Scussolini, V. Cavanni, G. Miraglia, A.D. Marchi, R. Ceravolo, Experimental identification of a bistable device for seismic energy dissipation, Mechanical Systems and Signal Processing 256 (2026) 114512. https://doi.org/10.1016/j.ymssp.2026.114512.
[12] K. Erazo, S. Nagarajaiah, An offline approach for output-only Bayesian identification of stochastic nonlinear systems using unscented Kalman filtering, Journal of Sound and Vibration 397 (2017) 222–240.
[13] A.F. Vakakis, O.V. Gendelman, L.A. Bergman, A. Mojahed, M. Gzal, Nonlinear targeted energy transfer: state of the art and new perspectives, Nonlinear Dynamics 108 (2022) 711–741.
[14] H. Zuo, S. Zhu, Bistable track nonlinear energy sinks with nonlinear viscous damping for impulsive and seismic control of frame structures, Engineering Structures 272 (2022) 114982.
[15] V. Cavanni, L. Scussolini, L. Caneparo, R. Ceravolo, Optimal Design of Bistable Meta-Panels for Energy Dissipation in Buildings Under Seismic Excitation, in: International Conference on Experimental Vibration Analysis for Civil Engineering Structures, Springer, 2025: pp. 761–769.
[16] X. Tan, B. Wang, L. Wang, S. Zhu, S. Chen, K. Yao, P. Xu, Effect of beam configuration on its multistable and negative stiffness properties, Composite Structures 286 (2022) 115308. https://doi.org/10.1016/j.compstruct.2022.115308.
[17] R.L. Harne, K.-W. Wang, Harnessing bistable structural dynamics: for vibration control, energy harvesting and sensing, John Wiley & Sons, 2017.
[18] K. Worden, E.J. Cross, A Tutorial on Data-Driven Methods in Nonlinear Dynamics, in: Society for Experimental Mechanics Annual Conference and Exposition, Springer, 2023: pp. 51–70.
[19] S.J. Julier, J.K. Uhlmann, Unscented filtering and nonlinear estimation, Proceedings of the IEEE 92 (2004) 401–422.
[20] E. Matta, R. Ceravolo, A. De Stefano, A. Quattrone, L. Zanotti Fragonara, Unscented Kalman Filter for Non-Linear Identification of a New Prototype of Bidirectional Tuned Vibration Absorber: A Numerical Investigation, KEM 569–570 (2013) 948–955. https://doi.org/10.4028/www.scientific.net/KEM.569-570.948.
[21] A.F. Villaverde, A. Barreiro, A. Papachristodoulou, Structural identifiability of dynamic systems biology models, PLoS Computational Biology 12 (2016) e1005153.

This work is licensed under CC BY 4.0

Media and Publishing Partner